Quality assessment of Outgoing Longwave Radiation (OLR) derived from INSAT-3D Imager: Impact of GSICS correction

AMIT KUMAR, VIRENDRA SINGH, SUNIL MUKHERJEE and RANDHIR SINGH*

India Meteorological Department, New Delhi – 110 003, India

**Space Applications Centre, ISRO, Ahmedabad, India*

(*Received 9 February 2018, Accepted 23 January2019*)

e mail : amitkumar.777@hotmail.com

सार – इनसैट-3 डी बहिर्गामी दीर्घतरंग विकिरण (OLR), पिक्सल विभेदन स्तर पर एक तेजी से वितरण स्तर-2 का उत्पाद है जो इनसैट-3 डी के इमेजर पेलोड से हर आधे घंटे पर प्राप्त करके प्रचालनात्मक रूप में तैयार किया जाता है। इसके साथ ही बहिर्गामी दीर्घ तरंग विकिरण के गुणनफल का दैनिक और मासिक उत्पाद तैयार किया जाता है। बहिर्गामी दीर्घतरंग विकिरण का आकलन इनसैट-3 डी इमेजर के इंफ्रारेड विंडोज (TIR1: 10.3-11.3 μm, TIR2: 11.5-12.5 μm) और जलवाष्प (WV: 6.5-7.1 μm) चैनल से विकिरित प्रेक्षणों से किया जाता है। इस अध्ययन में बहिर्गामी दीर्घतरंग विकिरण का आकलन फरवरी 2014 से दिसम्बर 2017 तक इनसैट-3 डी इमेजर विकिरित प्रेक्षण का उपयोग करके किया गया है जो CERES (पृथ्वी की विकीर्णन ऊर्जा प्रणाली, एन पी पी उपग्रह पर स्थापित से) से मान्य है। समरूप दृश्यों के लिए इनसैट-3 डी इमेजर से आकलित बहिर्गामी दीर्घतरंग विकिरण की चमक अच्छी गुणवत्ता की है जिसकी औसत सी सी 0.93 है, पूर्वाग्रह -5.03 Wm^{-2} और आर एम एस डी 10.39 Wm^{-2} है, और इसका उपयोग विभिन्न अनुप्रयोगों के अध्ययन में किया जा सकता है।

ABSTRACT. The INSAT-3D Outgoing longwave radiation (OLR), a fast-delivery level-2 product at pixel resolution, is being generated operationally from every half hourly acquisition of Imager Payload of INSAT-3D. In addition to this, binned daily and monthly OLR products are also generated. The OLR is estimated from the radiance observations in the infrared windows (TIR1: 10.3-11.3μm, TIR2: 11.5-12.5μm) and water vapor (WV: 6.5-7.1 μm) channels of INSAT-3D Imager. In the present study, OLR estimated using the INSAT-3D Imager radiance observation is validated with the CERES (Cloud and Earth's Radiant Energy System; on board NPP satellite) from February, 2014 to December, 2017. For the uniform scenes, OLR estimated using INSAT-3D Imager radiance is of good quality with mean CC 0.93, bias -5.03 Wm^{-2} & RMSD 10.39 Wm^{-2} and it could be used in the various applications studies.

Key words – OLR, Validation, INSAT-3D, CERES.

1. Introduction

Outgoing longwave radiation (OLR) is a major component of Earth's radiation budget and it represents the total amount of radiation emitted from earth-atmosphere system to the outer space. The top of the atmosphere radiative energy balance between net incoming solar radiation and OLR is crucial in determining the large-scale atmospheric circulation and, therefore, the synoptic evolution that is important for weather and climate prediction. Since long, OLR has been estimated for variety of problems in climate sensitivity and diagnostics (Schmetz and Liu, 1988), numerical weather forecasting and climate models. OLR varies inversely with the cloud top temperature resulting low radiation values from convective systems.

OLR has been estimated by satellite instruments since 1974 making it one the longest available satellite-based records for any geophysical parameters. Many dedicated broadband instruments are flown over satellites for measuring OLR like, Earth Radiation Budget Experiment (ERBE), Scanner Radiometer for Radiation Budget (ScaRab) and Cloud and Earth's Radiant Energy System (CERES) etc. In addition to these many algorithms are also developed for estimating OLR by converting the narrowband radiance observations into broadband flux (Gruber and Winston, 1978; Ellingson and Ferraro, 1983; Gruber and Krueger, 1984). Ellingson *et al*. (1989) have shown that the linear combination of only four (6.6-6.9 μm; 7.9-8.5 μm; 13.1-13.6 μm; 14.3-14.7 μm) High Resolution Infrared Sounder (HIRS) channels could account for more than 99% of the OLR total variance. Schmetz and Liu (1988) and Cheruy *et al*. (1991) developed OLR retrieval technique using two channels (infrared window and water vapor) of Meteosat. Minnis *et al*. (1991) developed an algorithm to estimate OLR using Geostationary Operational Environmental Satellite (GOES) imager window channels with additional water vapor information from analysis.

Ba and Ellingson (2001) estimated OLR using several channels of the GOES sounder and presented comparisons with the CERES measurements. Ba *et al*. (2003) and Lee *et al*. (2004) adapted the HIRS OLR technique to GOES sounder. Singh *et al*. (2007) estimated OLR using the infrared window and water vapor channels radiances from Kalpana satellite. Various studies (Ellingson *et al*., 1994; Gruber *et al*., 1994; Lee *et al*., 2007) have been caries out to validate these OLR estimates with broadband observations obtained from ERBE and CERES.

INSAT-3D satellite (positioned 82° E), launched into a Geosynchronous Transfer Orbit (GTO) by Ariane-5 VA-214 launch vehicle from Kourou, French Guiana on 26th July, 2013. INSAT-3D has four payloads, two meteorological payloads namely: Six channel Imager, Nineteen channels IR Sounder, One Data Relay Transponder and One Satellite Aided Search and Rescue (Table 1). The INSAT-3D imager provides imaging capability of the earth disc from geostationary altitude in one visible (VIS) (0.55-0.75μm) and five infrareds; Short-Wave Infrared (SWIR) (1.55-1.70 μm), Mid-Infrared (MIR) (3.80-4.00 μm), Water Vapour (WV) (6.5-7.1μm), Thermal Infrared-1 (TIR1) (10.2-11.3μm) and Thermal Infrared-2 (TIR-2) (11.5-12.5 μm) bands. The ground resolution at the sub-satellite point is nominally 1 km × 1 km for VIS and SWIR bands, 4 km × 4 km for one MIR and both TIR bands and 8 km × 8 km for WV band (Table 1). The primary goal of this study is to evaluate the performance of INSAT-3D satellite derived Outgoing longwave radiation. This is achieved by comparing INSAT derived Outgoing longwave radiation against Clouds and the Earth's Radiant Energy System (CERES) on board Suomi NPP (National Polar-orbiting Partnership) for the period February 2014 to December 2017. In addition, a preliminary evaluation of the impact of Global Space-based Inter-Calibration System (GSICS) correction on the quality of INSAT-3D satellite derived Outgoing longwave radiation is also carried out.

2.   Data and methodology

2.1. *INSAT-3D OLR data*

INSAT-3D Outgoing longwave radiation (OLR) is generated operationally at INSAT Meteorological Data Processing System (IMDPS), New Delhi at pixel resolution and at half-hourly interval. OLR is estimated from narrow band radiances from WV (6.5-7.1 μm), TIR-1 (10.2-11.3 μm) and TIR-2 (11.5-12.5 μm) channels of INSAT-3D imager (Singh *et al*., 2013; OLR ATBD10.19038/SAC/10/3DIMG_L2B_OLR). The product dimension is 20° E to 130° E and 60° S to 60° N.

Channel ID	Channel name	Spectral range (μm)	Resolution (km)
TIR 1	Long Wave Infrared	10.2-11.3	4.0
TIR 2	Split	11.5-12.5	4.0
WV	Water Vapor	6.5-7.1	8.0
MIR	Medium Wave Infrared	3.8-4.0	4.0
SWIR	Short Wave Infrared	1.55-1.70	1.0
VIS	Visible	0.55-0.75	1.0

2.2. *Clouds and the Earth's Radiant Energy System (CERES) data*

The Clouds and the Earth's Radiant Energy System is a key instrument [Flight Model (FM) 5] is placed on board the Suomi National Polar-orbiting Partnership (NPP) satellite on October 28, 2011. Data available from this CERES instrument is used in this study. CERES climate data records involve an unprecedented level of data fusion: CERES measurements are combined with imager data (e.g., MODIS on Terra and Aqua, VIIRS on S-NPP), 4-D weather assimilation data, microwave sea-ice observations and measurements from five geostationary satellites to produce climate-quality radiative fluxes at the top-of-atmosphere, within the atmosphere and at the surface, together with the associated cloud and aerosol properties. CERES data has gone through extensive validation of both TOA and surface radiation using TOA consistency tests and direct comparisons of surface fluxes with ground-based measurements over both land and ocean. The TOA fluxes are a factor of 2-3 better than Earth Radiation Budget Experiment (ERBE) and the flux record is highly stable. The CERES OLR datasets have a horizontal resolution (at nadir) of 20 Km. Suomi-NPP, CERES data (CER_ES8_NPP-FM5_Edition1-CV) for the period February 2014 to December 2017 is downloaded from earthdata.nasa.gov webpage. For the month of October, 2017, the data is not available on the said webpage.

2.3. *Data selections criteria*

To generate collocated dataset, INSAT-3D OLR was averaged for 3 × 3 pixels to match the CERES (about 20 km nadir) resolution and uniform scenes are used. The uniform scenes have small spatial variation and are measured by the coefficient of variation (CV) of INSAT-3D OLR. The CV is defined as the ratio of the standard deviation of INSAT-3D OLR to its mean value
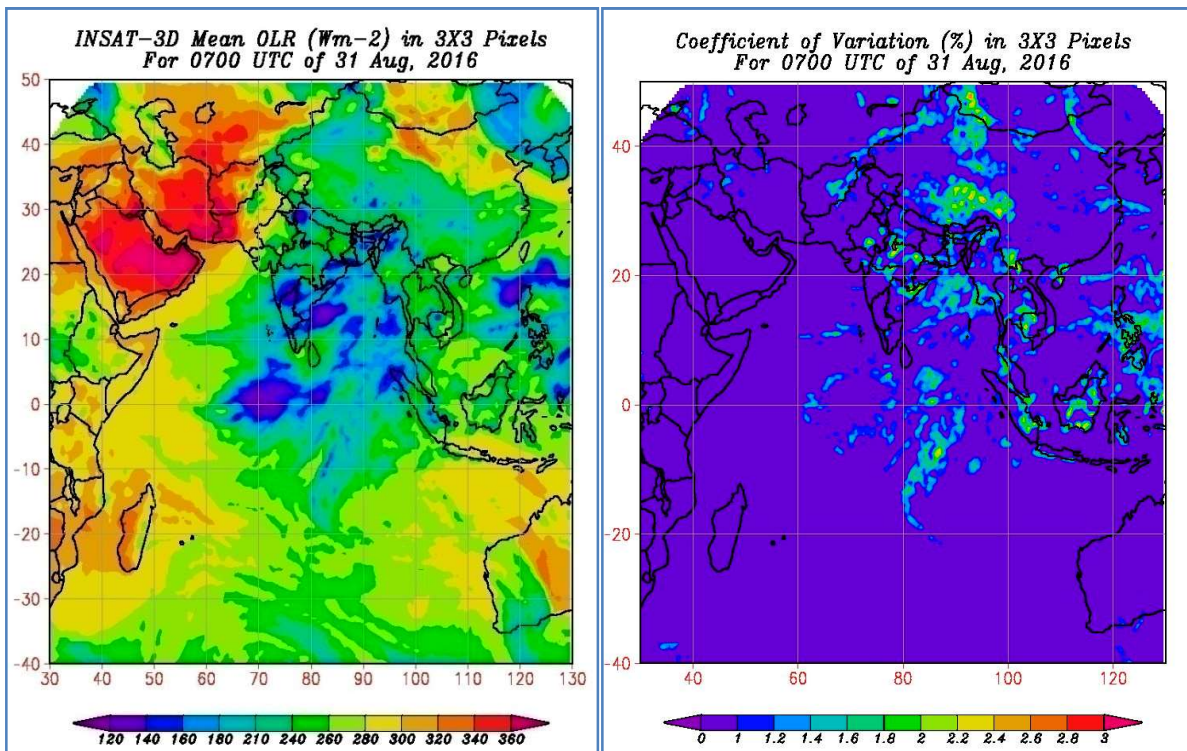
Fig. 1. INSAT-3D mean OLR (Wm^{-2}) in 3 × 3 pixels (upper panel) and coefficient of variation (%) in 3 × 3 pixels (lower panel), 0700 UTC 31 August, 2016

in 3 × 3 pixels for comparison with CERES. If the standard deviation of INSAT-3D OLR in 3 × 3 pixels is less than 1% of its mean value, the scene is judged to be uniform. As an example, Fig.1 shows the spatial distribution of the mean and CV of OLR in 3 × 3 pixels, at 0700 UTC 31st August, 2016. Over most part of the domain the value of CV is less than 1%, except around the cloud edges where higher value of CV is seen. Finally, only those CERES observations which were obtained within ±5 minutes and 5 km radius of the INSAT-3D OLR were considered. Based on above criteria collocated points were obtained for each month. The validation is done over the region from 30° E to 130° E and 50° N to 40° S. The differences between the INSAT 3D OLR and NPP CERES OLR are calculated for each collocated point on monthly basis and are categorized in the range ±5 Wm^{-2} to ±20 Wm^{-2}. The statistical parameters are obtained for uniform scenes.

3. Results and discussion

3.1. *Inter-comparison of INSAT-3D and CERES OLR*

For comparing the satellite derived Outgoing longwave radiation from a geostationary platform and a polar platform, *i.e.*, Imager payload onboard INSAT-3D

satellite and CERES payload on Suomi NPP satellite, special care is taken while preparing collocated dataset. This is mainly because of the difference in spatial and temporal resolution of both the satellites. Hence as mentioned in above section, uniform scenes are used and collocated dataset is prepared subject to satisfying the above-mentioned data selection criteria.

3.1.1. *2D- Density plots*

Fig. 2 shows the comparison, using density plots, between the CERES and INSAT-3D derived OLR products for different seasons. From the density plots it can be concluded that almost all points are lying on or below the line of unity referring to a very good correlation between INSAT-3D and CERES derived OLR products. It can be seen that INSAT-3D derived OLR is showing a negative bias (*i.e.*, underestimation by INSAT-3D) throughout the study period. While interpreting the results it should be kept in mind that the OLR data available from INSAT-3D is at a better resolution then CERES derived OLR and it is averaged for collocation purpose. Hence, INSAT-3D derived OLR has a good potential in using this dataset for climatological purposes to further assess the performance of INSAT-3D derived OLR statistical skill scores are also worked out.
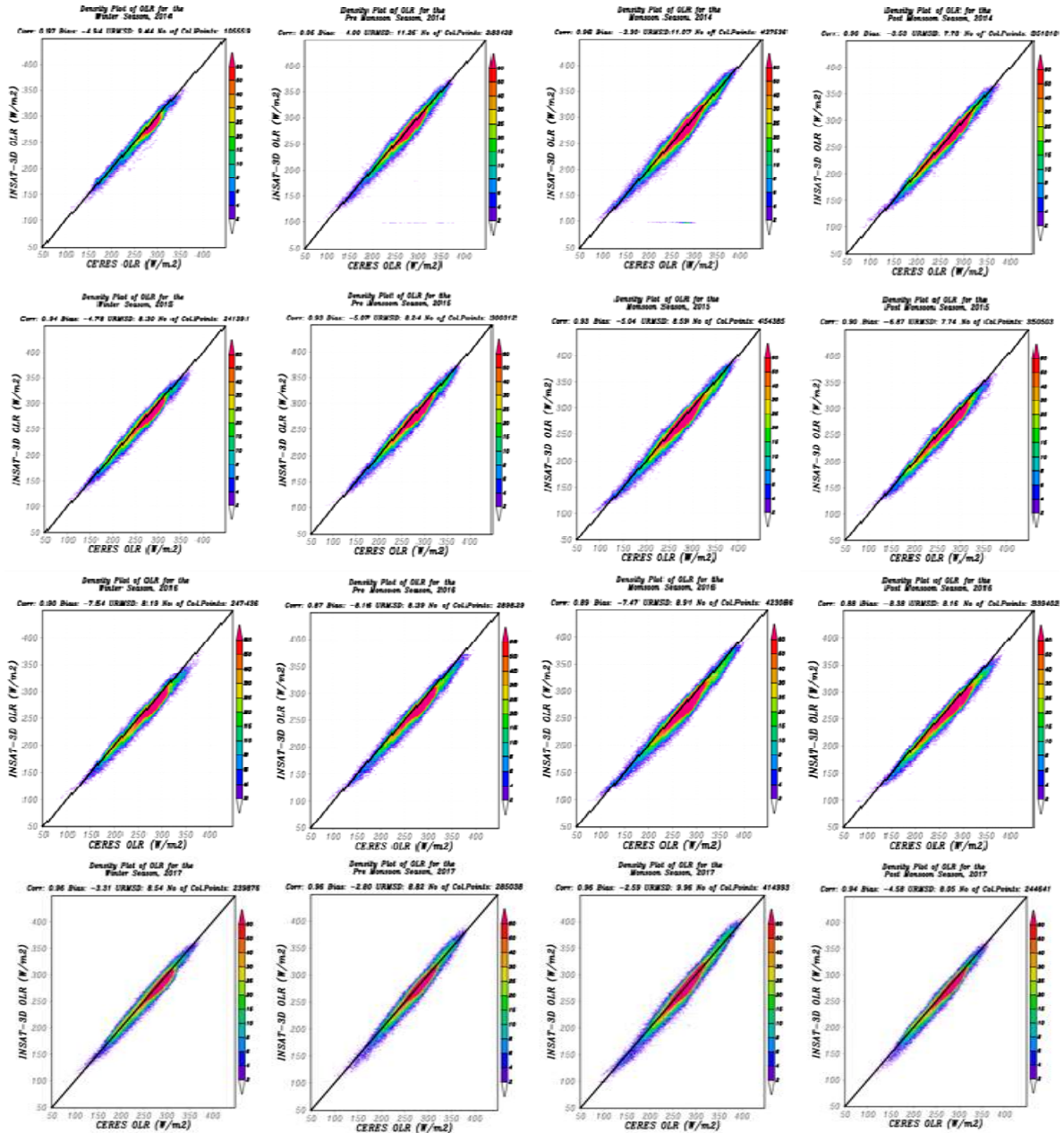
Fig. 2. Seasonal density plots between INSAT-3D, Imager OLR and Suomi-NPP, CERES OLR (February 2014 to December 2017)

3.1.2. *Statistical skill scores*

The collocated gridded comparison statistics are used to evaluate the performance of INSAT-3D OLR product. For quantitative evaluation, following widely applied statistical metrices are used: Linear correlation coefficient (CC), Standard Deviation (SD), Bias, Root Mean Square deviation (RMSD), Bias Corrected Root Mean Square Deviation (URMSD). The statistical metrices are computed as follows:

$$\text{Bias} = \frac{1}{N}\sum_{i=1}^{N}(A)_i - (B)_i \tag{1}$$

$$\text{SD} = \sqrt{\left\{\frac{[N\sum_{i=1}^{N}(A_i - \overline{A})^2][N\sum_{i=1}^{N}(B_i - \overline{B})^2]}{N}\right\}} \tag{2}$$
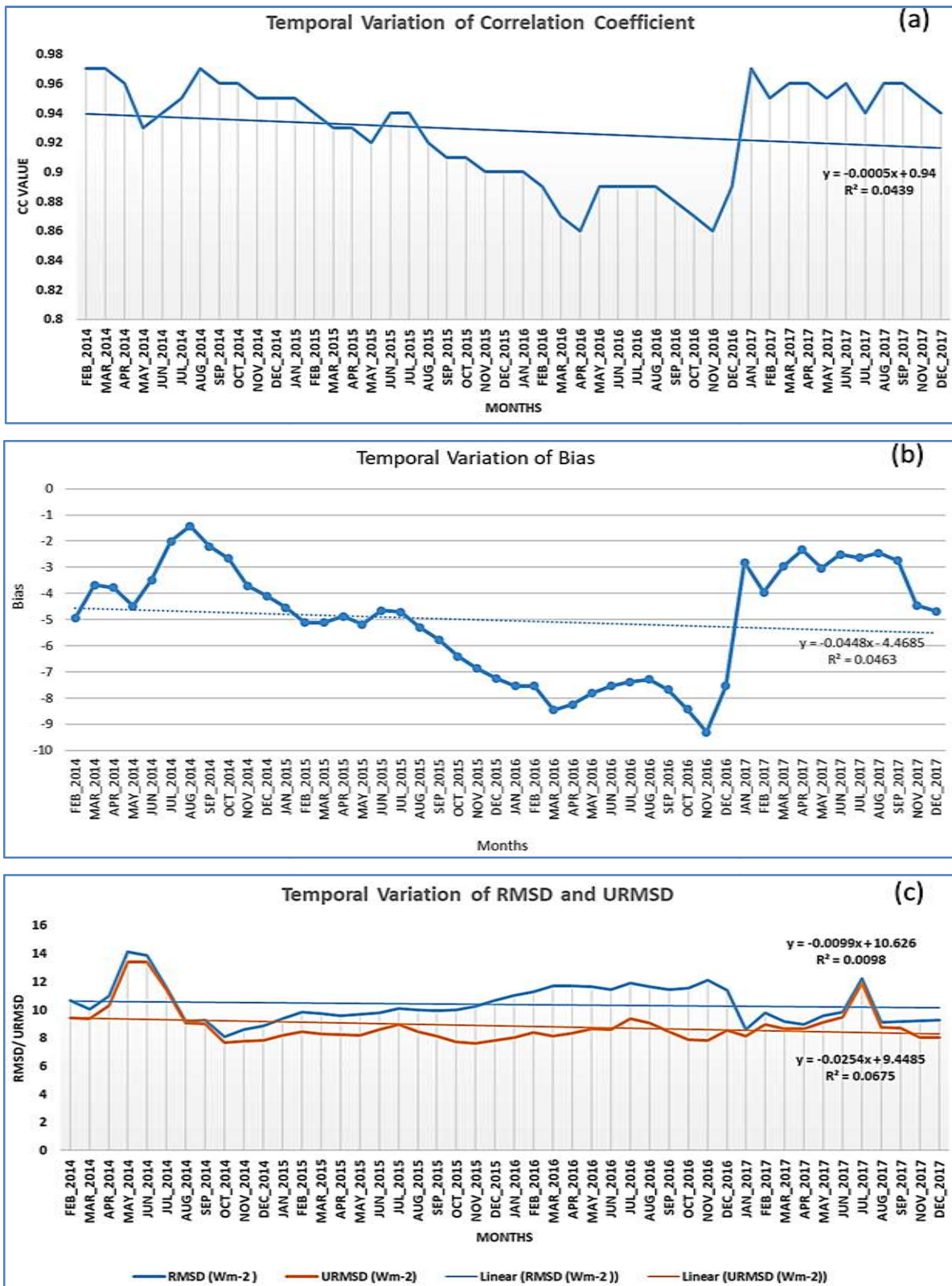
Figs. 3(a-c). (a)Monthly correlation coefficient, (b) Monthly bias and (c) Monthly RMSD & URMSD between INSAT-3D, Imager OLR and Suomi-NPP, CERES OLR

TABLE 2

Validation statistics from February 2014 to December 2017 on monthly basis

Month	Collocated Points	Correlation Coefficient	Bias (Wm^{-2})	RMSD (Wm^{-2})	URMSD (Wm^{-2})	Mean INSAT-3D OLR(Wm^{-2})	Mean CERES OLR (Wm^{-2})
Feb 2014	105559	0.97	-4.94	10.66	9.44	265.53	270.46
Mar 2014	97225	0.97	-3.68	10.06	9.37	271.94	275.62
Apr 2014	84122	0.96	-3.78	10.96	10.29	276.9	280.68
May 2014	102081	0.93	-4.48	14.15	13.42	272.37	276.85
Jun 2014	112906	0.94	-3.48	13.86	13.42	275.17	278.65
Jul 2014	126337	0.95	-2.01	11.6	11.43	272.63	274.64
Aug 2014	102467	0.97	-1.42	9.16	9.05	276.8	278.22
Sep 2014	85826	0.96	-2.21	9.29	9.03	279.2	281.41
Oct 2014	107902	0.96	-2.66	8.11	7.67	274.16	276.82
Nov 2014	114748	0.95	-3.7	8.6	7.76	265.09	268.79
Dec 2014	129168	0.95	-4.1	8.84	7.83	262.88	266.98
Jan 2015	137500	0.95	-4.54	9.36	8.19	265.28	269.82
Feb 2015	103891	0.94	-5.11	9.86	8.44	267.73	272.84
Mar 2015	103333	0.93	-5.11	9.75	8.3	271.27	276.39
Apr 2015	82078	0.93	-4.87	9.57	8.24	274.11	278.99
May 2015	114901	0.92	-5.18	9.7	8.2	272.33	277.51
Jun 2015	122422	0.94	-4.65	9.78	8.6	271.7	276.35
Jul 2015	134897	0.94	-4.71	10.12	8.96	272.85	277.56
Aug 2015	103272	0.92	-5.3	9.98	8.46	276.32	281.61
Sep 2015	93794	0.91	-5.76	9.96	8.12	276.25	282
Oct 2015	98792	0.91	-6.4	10.01	7.71	271.2	277.59
Nov 2015	117251	0.9	-6.86	10.25	7.62	264.55	271.4
Dec 2015	134460	0.9	-7.24	10.68	7.85	261.25	268.49
Jan 2016	136500	0.9	-7.54	11.01	8.02	259.34	266.89
Feb 2016	110936	0.89	-7.53	11.28	8.39	266.66	274.2
Mar 2016	102756	0.87	-8.45	11.73	8.13	269.27	277.72
Apr 2016	81595	0.86	-8.24	11.71	8.32	272.22	280.46
May 2016	105478	0.89	-7.81	11.67	8.67	269.36	277.17
Jun 2016	118761	0.89	-7.54	11.45	8.61	266.47	274.01
Jul 2016	118691	0.89	-7.38	11.93	9.38	265.85	273.22
Aug 2016	95540	0.89	-7.28	11.63	9.07	271.59	278.87
Sep 2016	90094	0.88	-7.68	11.43	8.46	274.25	281.93
Oct 2016	84137	0.87	-8.42	11.53	7.88	270.04	278.47
Nov 2016	119860	0.86	-9.3	12.14	7.81	262.87	272.16
Dec 2016	135405	0.89	-7.54	11.39	8.54	263.92	271.46
Jan 2017	134388	0.97	-2.81	8.62	8.15	266.52	269.32
Feb 2017	105488	0.95	-3.96	9.8	8.97	268.06	272.02
Mar 2017	96495	0.96	-2.97	9.15	8.66	272.85	275.82
Apr 2017	84428	0.96	-2.33	8.95	8.64	280.11	282.43
May 2017	104115	0.95	-3.04	9.59	9.1	275.67	278.7
Jun 2017	110112	0.96	-2.51	9.82	9.49	274.5	277.01
Jul 2017	120680	0.94	-2.64	12.21	11.92	272.01	274.66
Aug 2017	94478	0.96	-2.46	9.11	8.77	276.65	279.11
Sep 2017	89723	0.96	-2.74	9.15	8.73	278.85	281.59
Nov 2017	116328	0.95	-4.46	9.21	8.06	266.37	270.82
Dec 2017	128313	0.94	-4.68	9.3	8.04	264.42	269.11
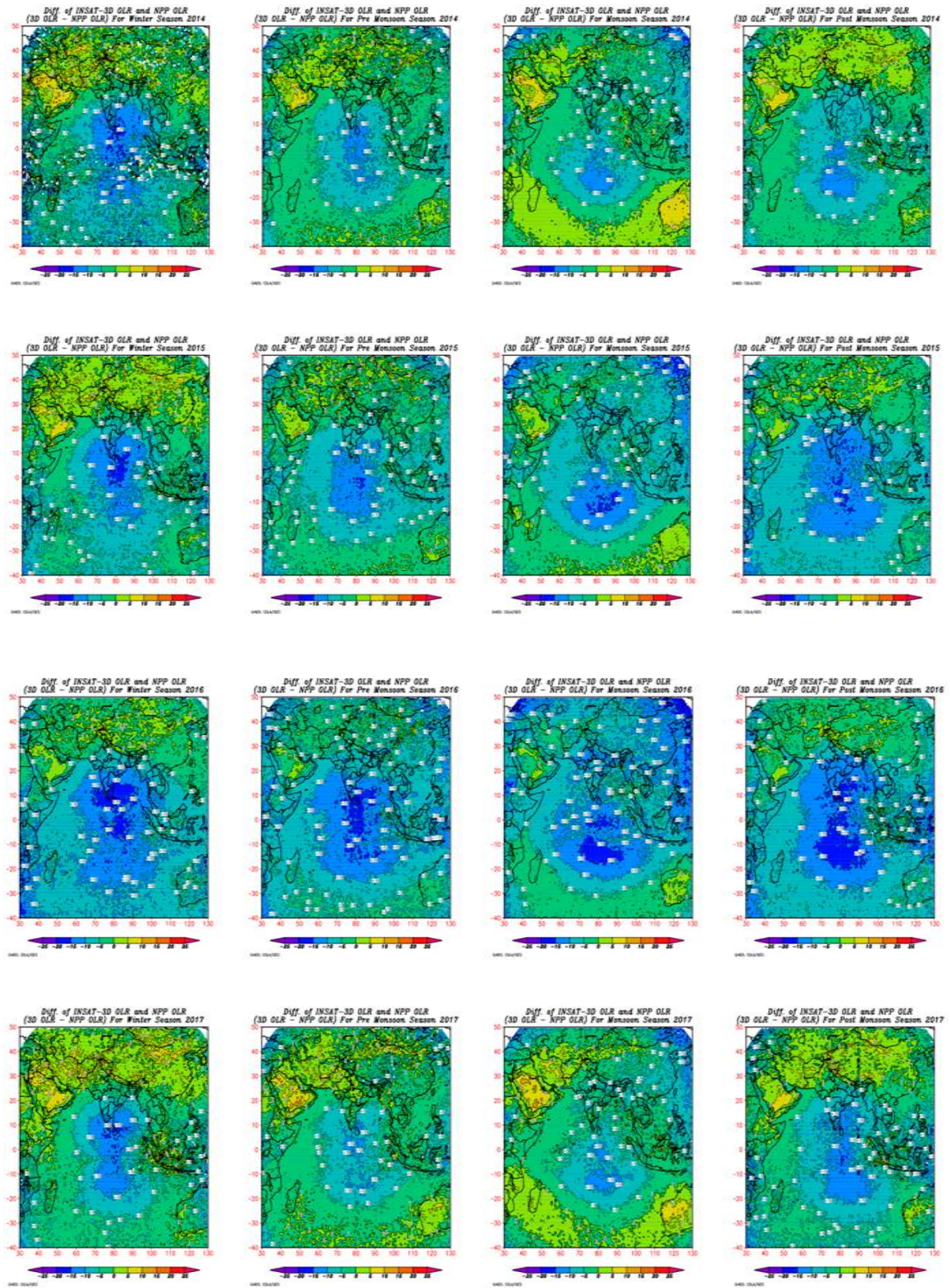
Fig. 4. Monthly Bias Plots between INSAT-3D, Imager OLR and Suomi-NPP, CERES OLR (February 2014 to December 2017)

$$CC = \frac{N(\sum_{i=1}^{N} A_i B_i) - (\sum_{i=1}^{N} A_i)(\sum_{i=1}^{N} B_i)}{\sqrt{[N \sum_{i=1}^{N} A^2_i - (\sum_{i=1}^{N} A_i)^2][N \sum_{i=1}^{N} B^2_i - (\sum_{i=1}^{N} B_i)^2]}} \qquad (3)$$

$$RMSD = \sqrt{\frac{1}{N} \sum_{i=1}^{N} (A_i - B_i)^2} \qquad (4)$$

$$URMSD = \sqrt{RMSD^2 - BIAS^2} \qquad (5)$$

where, A is OLR derived using INSAT 3D, B is OLR derived using CERES and N is the number of samples.

Bias refers to the tendency of INSAT-3D derived OLR to over- or under-estimate with respect to that of CERES derived OLR. Standard Deviation tell us how the measurements of OLR from INSAT-3D are spread out from that of CERES. Correlation coefficient represents the linear interdependence of two datasets. It lies between +1 to -1. RMSD is a measure of accuracy. Larger errors (*i.e.*, deviations of INSAT-3D derived OLR from CERES OLR) will have a disproportionately large effect on RMSD.

The monthly correlation coefficient for the period February, 2014 to December, 2017 is shown in Fig. 3(a). The datasets exhibit a strong correlation throughout the period with a mean correlation of 0.93. It can be clearly seen from the Fig. 3(a) that, the quality of INSAT-3D derived OLR showed continuous degradation over the period with reaching a Minimum of 0.86 in April, 2016. However, after the application of GSICS correction in December, 2016, the quality of the product has shown improvement.

The collocated gridded comparison statistics (no. of collocated points, CC, Bias, RMSD, URMSD) for each month are shown in Table 2 and Fig. 3 respectively. It can be clearly seen from Table 2 that the Bias has increased from minimum bias of -1.42 Wm^{-2} in August, 2014 to -9.3 Wm^{-2} in November, 2016 which is maximum bias observed during the study period. The monthly bias maps at pixel level are also shown in Fig. 4 from February, 2014 to December, 2017. It can be seen from the bias maps that at sub-satellite point of INSAT-3D, it is under estimating consistently with a negative bias of -10 to -15 Wm^{-2}. However, this negative bias goes on decreasing when we move away from the sub-satellite point and changes to positive bias over landmass. Similarly, RMSD has also shown increasing trend over the months from February, 2014 to November, 2016 with values in the range 8.6 to 14.15 Wm^{-2}. Season-wise statistics are shown in Table 4.

This underestimation of OLR by INSAT-3D when compared to the CERES could be due to the biases in the INSAT-3D radiances. Singh *et al*. (2015) compared the INSAT-3D observed radiances with radiative transfer model simulated radiances using NCEP and ECMWF analyzed atmospheric state. They found a cold bias (as large as 2.5 K) in the thermal channels (TIR1 and TIR2) of INSAT-3D imager. Similarly, in another study, Singh *et al*. (2016) compared the INSAT-3D radiances (TIR1 and TIR2) with similar channels (bands 31 and 32) of MODIS and noticed a cold bias of the order of 2.5 to 3.5 K in INSAT-3D imager radiances. Therefore, INSAT-3D can underestimate the OLR due these cold biases in the thermal radiances.

To further investigate the quality of INSAT-3D OLR with respect to CERES OLR, the percentage of collocated points with biases ranging from -20 Wm^{-2} to 20 Wm^{-2} are calculated as shown in Fig. 5(a) and Table 3. The purpose of this segregation is to get a fair amount of idea of the nature and amount of biases which are dominating the overall bias as shown in Fig. 5(b) with number of collocated points on the extremes. It can be clearly seen from the figure that the number of collocated points between -5 Wm^{-2} to 5 Wm^{-2} were showing a declining trend whereas the number of collocated points <-20 Wm^{-2} and >20 Wm^{-2} were showing an increasing trend till December, 2016. This further points to regular updating of radiance calibration coefficient values of INSAT-3D Imager in processing chain.

3.2. *Impact of GSICS correction on the quality of INSAT-3D derived Outgoing longwave radiation*

The INSAT-3D radiance coefficients were updated for the first time, in processing chain of INSAT-3D on 23rd December, 2016, at INSAT Meteorological Data Processing System (IMDPS), New Delhi, using GSICS correction carried out at Space application Centre, ISRO Ahmedabad. GSICS is an international collaborative effort initiated in 2005 by WMO and the CGMS to monitor, improve and harmonize the quality of observations from operational weather and environmental satellites of the Global Observing System (GOS). GSICS aims at ensuring consistent accuracy among space-based observations worldwide for climate monitoring, weather forecasting and environmental application (http://gsics.wmo.int/). It can be clearly seen from Fig. 3 and Fig. 5(b) that after applying GSICS correction, the quality of INSAT-3D derived OLR has shown improvement. It can be clearly seen from the Figs. 3&4 and Table 2 that after implementation of GSICS correction, the Bias has come down from -7.54 Wm^{-2} in December 2016 to -2.81 Wm^{-2} in January 2017. Similarly, RMSD came down from 11.39 Wm^{-2} in December 2016 to 8.62 Wm^{-2} in January 2017.
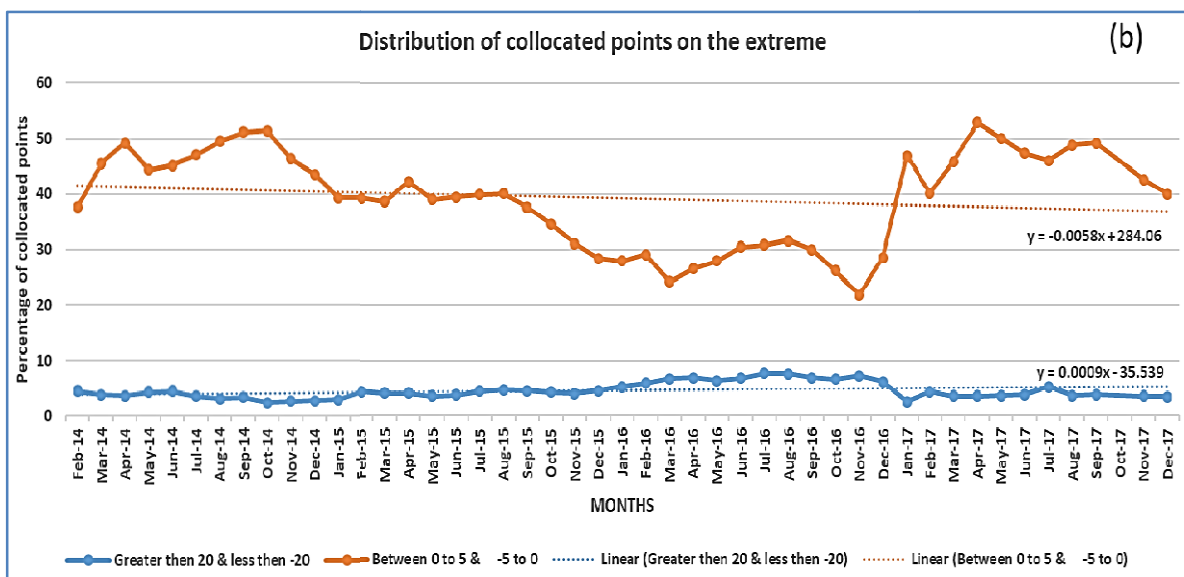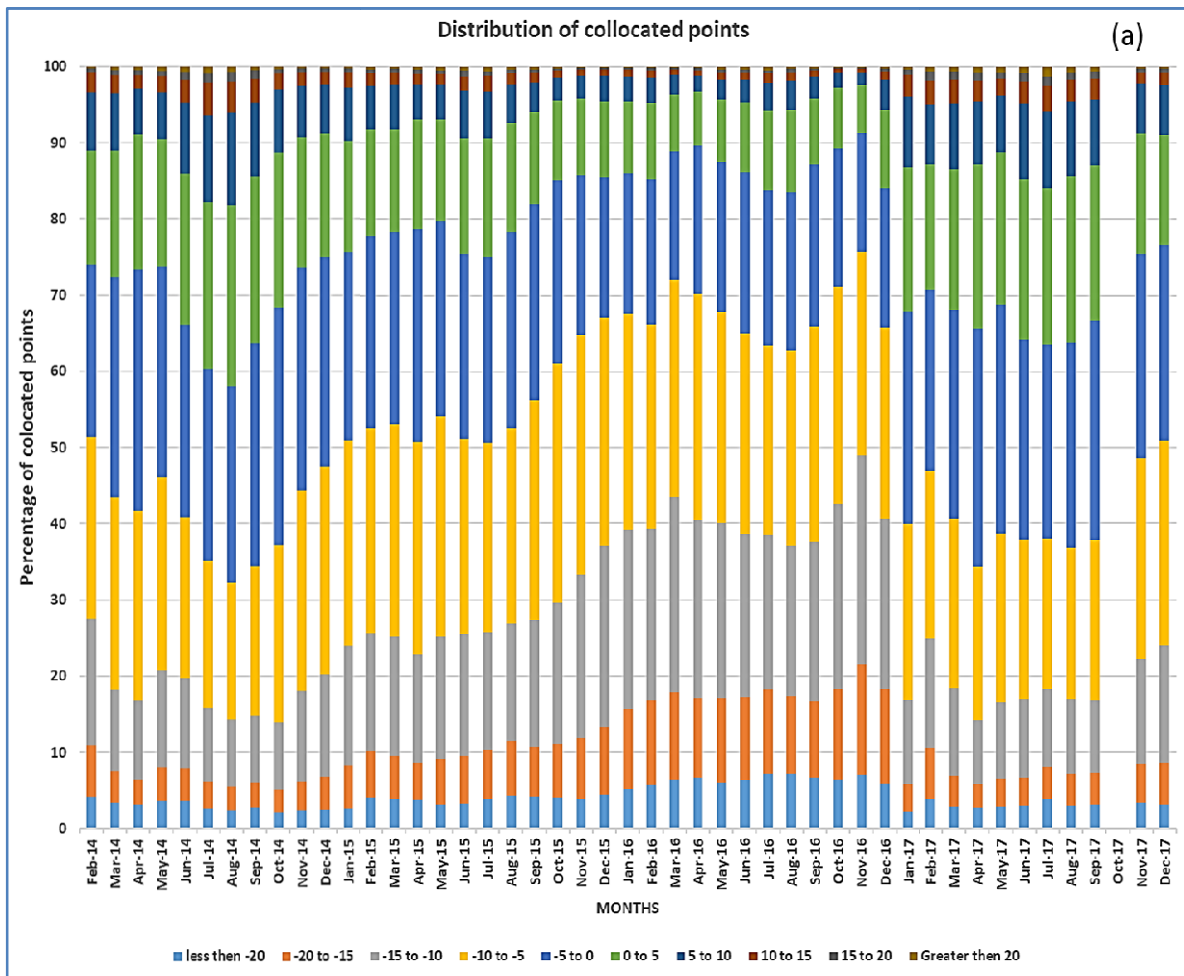
Figs. 5(a&b). (a) Percentage of collocated points with biases ranging from -20 Wm^{-2} to 20 Wm^{-2} (b) Temporal variation in percentage of collocated points with biases on the extremes: < -20 Wm^{-2} & >20 Wm^{-2} and -5 Wm^{-2} to 5 wm^{-2}

TABLE 3

Percentage of collocated points from INSAT-3D w.r.t. CERES in terms of Bias (Wm^{-2}) from February 2014 to December 2017

Month	less than -20	-20 to -15	-15 to -10	-10 to -5	-5 to 0	0 to 5	5 to 10	10 to 15	15 to 20	Greater than 20	Greater than 20 & less than -20	Between 0 to 5 & -5 to 0
Feb 14	4.18	6.78	16.62	23.79	22.54	15.01	7.76	2.43	0.61	0.27	4.45	37.55
Mar14	3.34	4.15	10.83	25.2	28.81	16.68	7.46	2.37	0.69	0.47	3.81	45.49
Apr 14	3.12	3.4	10.23	24.94	31.65	17.64	6.07	1.82	0.65	0.48	3.6	49.29
May14	3.65	4.43	12.72	25.29	27.61	16.76	6.14	2.05	0.73	0.62	4.27	44.37
Jun 14	3.64	4.36	11.71	21.08	25.22	19.92	9.24	3.11	0.98	0.76	4.4	45.14
Jul 14	2.66	3.44	9.78	19.2	25.26	21.81	11.43	4.17	1.32	0.92	3.58	47.07
Aug14	2.39	3.17	8.87	17.81	25.74	23.8	12.1	4.13	1.24	0.73	3.12	49.54
Sep 14	2.81	3.19	8.81	19.58	29.28	21.84	9.66	3.23	1.06	0.55	3.36	51.12
Oct 14	2.1	2.96	8.91	23.18	31.22	20.21	8.39	2.11	0.6	0.32	2.42	51.43
Nov 14	2.38	3.8	11.87	26.33	29.22	17.07	6.8	1.75	0.5	0.28	2.66	46.29
Dec 14	2.45	4.33	13.39	27.36	27.45	16.12	6.5	1.65	0.47	0.27	2.72	43.57
Jan 15	2.66	5.62	15.75	26.9	24.72	14.6	6.93	1.99	0.52	0.3	2.96	39.32
Feb 15	4.05	6.1	15.49	26.97	25.17	14.07	5.59	1.71	0.52	0.32	4.37	39.24
Mar 15	3.82	5.71	15.6	28	25.32	13.34	5.87	1.59	0.47	0.28	4.1	38.66
Apr 15	3.69	4.82	14.34	27.86	28.05	14.3	4.56	1.41	0.56	0.41	4.1	42.35
May15	3.15	5.89	16.13	28.95	25.69	13.33	4.49	1.42	0.5	0.44	3.59	39.02
Jun 15	3.22	6.36	15.92	25.61	24.29	15.16	6.26	1.94	0.72	0.51	3.73	39.45
Jul 15	3.81	6.57	15.32	24.93	24.46	15.45	6.22	2.02	0.64	0.59	4.4	39.91
Aug15	4.32	7.12	15.42	25.73	25.84	14.26	5.02	1.43	0.49	0.36	4.68	40.1
Sep 15	4.21	6.49	16.63	29.01	25.69	12.01	3.96	1.25	0.42	0.32	4.53	37.7
Oct 15	4.05	6.99	18.53	31.41	24.17	10.51	2.96	0.87	0.28	0.22	4.27	34.68
Nov 15	3.88	7.95	21.49	31.45	21	10.09	3.01	0.72	0.24	0.16	4.04	31.09
Dec 15	4.41	8.95	23.73	29.99	18.49	9.92	3.38	0.75	0.22	0.16	4.57	28.41
Jan 16	5.12	10.47	23.68	28.28	18.46	9.47	3.2	0.9	0.25	0.17	5.29	27.93
Feb 16	5.67	11.09	22.57	26.8	19.16	9.93	3.36	0.96	0.28	0.19	5.86	29.09
Mar 16	6.49	11.36	25.68	28.63	16.84	7.34	2.55	0.68	0.25	0.18	6.67	24.18
Apr 16	6.68	10.43	23.28	29.74	19.51	7.07	2.09	0.75	0.25	0.21	6.89	26.58
May16	6.01	11.07	22.93	27.78	19.65	8.27	2.65	0.91	0.4	0.33	6.34	27.92
Jun 16	6.37	10.85	21.29	26.48	21.26	9.19	2.93	0.9	0.37	0.35	6.72	30.45
Jul 16	7.21	10.9	20.29	25.01	20.41	10.39	3.69	1.22	0.42	0.48	7.69	30.8
Aug16	7.2	10.12	19.75	25.74	20.68	10.9	3.85	1.05	0.4	0.32	7.52	31.58
Sep 16	6.67	10	20.87	28.37	21.27	8.7	2.8	0.85	0.26	0.21	6.88	29.97
Oct 16	6.5	11.72	24.36	28.5	18.26	7.88	2.01	0.48	0.17	0.11	6.61	26.14
Nov 16	7.08	14.35	27.53	26.8	15.57	6.28	1.68	0.43	0.15	0.13	7.21	21.85
Dec 16	5.91	12.34	22.37	25.18	18.24	10.33	4.01	1.07	0.33	0.22	6.13	28.57
Jan 17	2.17	3.62	11.09	23.02	27.96	18.96	9.26	2.82	0.72	0.38	2.55	46.92
Feb 17	3.8	6.84	14.27	22.06	23.76	16.44	7.9	3.16	1.22	0.57	4.37	40.2
Mar 17	2.96	3.94	11.5	22.26	27.44	18.45	8.56	3.24	1.09	0.55	3.51	45.89
Apr 17	2.83	2.99	8.29	20.19	31.37	21.52	8.34	2.69	1.07	0.7	3.53	52.89
May17	2.97	3.59	9.95	22.2	30.07	20.12	7.32	2.29	0.8	0.68	3.65	50.19
Jun 17	2.99	3.67	10.33	20.93	26.3	21.07	9.83	3.03	1.01	0.84	3.83	47.37
Jul 17	3.87	4.15	10.2	19.73	25.53	20.52	10.13	3.36	1.18	1.34	5.21	46.05
Aug17	3	4.17	9.84	19.78	26.93	21.95	9.78	2.87	1.01	0.67	3.67	48.88
Sep 17	3.17	4.06	9.55	20.92	29.03	20.25	8.7	2.81	0.88	0.61	3.78	49.28
Nov 17	3.33	5.11	13.78	26.4	26.83	15.83	6.46	1.55	0.46	0.25	3.58	42.66
Dec 17	3.17	5.32	15.51	26.97	25.59	14.43	6.6	1.68	0.46	0.26	3.43	40.02

TABLE 4

Validation statistics from February 2014 to December 2017 on seasonal basis

Month	Correlation Coefficient	Bias (Wm^{-2})	RMSD (Wm^{-2})	URMSD (Wm^{-2})	Mean INSAT-3D OLR (Wm^{-2})	Mean CERES OLR (Wm^{-2})
OLR_WINTER_2014	0.97	-4.94	10.66	9.44	265.53	270.46
OLR_PRE_MONSOON_2014	0.95	-4	11.94	11.25	273.57	277.56
OLR_MONSOON_2014	0.96	-2.3	11.31	11.07	275.63	277.92
POST_MONSOON_2014	0.96	-3.53	8.54	7.78	267.06	270.59
OLR_WINTER_MON_2015	0.94	-4.78	9.58	8.3	266.33	271.12
OLR_PRE_MONSOON_2015	0.93	-5.07	9.68	8.24	272.45	277.53
OLR_MONSOON_2015	0.93	-5.04	9.96	8.59	274.02	279.08
OLR_POST_MONSOON_2015	0.9	-6.87	10.35	7.74	265.16	272.03
OLR_WINTER_MON_2016	0.9	-7.54	11.13	8.19	262.63	270.17
OLR_PRE_MONSOON_2016	0.87	-8.16	11.7	8.39	270.13	278.3
OLR_MONSOON_2016	0.89	-7.47	11.62	8.91	269.1	276.57
OLR_POST_MONSOON_2016	0.88	-8.38	11.7	8.16	265.07	273.44
OLR_WINTER_MON_2017	0.96	-3.31	9.16	8.54	267.2	270.51
OLR_PRE_MONSOON_2017	0.96	-2.8	9.26	8.82	276.03	278.83
OLR_MONSOON_2017	0.96	-2.59	10.29	9.96	275.21	277.79
OLR_POST_MONSOON_2017	0.94	-4.58	9.26	8.05	265.35	269.92

In terms of number of collocated points exhibiting biases, as shown in Figs. 5(a&b) and Table 3, it can be clearly seen that the number of collocated points between -5 Wm^{-2} to 5 Wm^{-2} increased from 22% in November 2016 to 53% in April 2017 and the number of collocated points having biases less than -20 Wm^{-2} and greater than 20 Wm^{-2} decreased from 7% in November 2016 to 2% in January 2017.

The effect of GSICS correction sustained till April 2017, after that, INSAT-3D, Imager derived OLR again started showing degradation trend. Therefore, it is suggested that the GSICS correction is applied at regular intervals, to maintain the quality of product.

5. Summary and conclusions

This paper evaluated the performance of INSAT-3D derived Outgoing Longwave Radiation, generated from operational IMDPS, New Delhi with Suomi-NPP, CERES derived Outgoing Longwave Radiation product over the domain from 30° E to 130° E and 50° N to 40° S during July 2014 to July 2017. For the uniform scenes, the bias between CERES and INSAT-3D OLR lies in the range of -1.42 to -9.3 Wm^{-2}, the correlation coefficient lies in the range 0.86 to 0.97 and RMSD lies in the range of 8.11 to 12.21 Wm^{-2}. The validation results suggest that the OLR estimated using INSAT-3D Imager radiance is of good quality (with mean CC 0.92, bias -5.32 Wm^{-2}, RMSD 10.31 Wm^{-2} & URMSD 8.58 Wm^{-2}). To facilitate comparison between the INSAT 3D OLR and CERES

OLR, the INSAT-3D OLR was averaged over 3 × 3 pixels which otherwise offers a better resolution at 8 km per pixel at nadir. The decreasing trend in quality of INSAT-3D OLR with respect to CERES OLR could be attributed to the radiances calibration is suggested. After applying GSICS correction in INSAT-3D radiance coefficient, the quality of INSAT-3D derived OLR has shown improvement. Therefore, it is suggested that the GSICS correction need to be applied at regular intervals to maintain the accuracy and quality of product. This small difference between the INSAT-3D OLR and CERES OLR suggest that the INSAT-3D derived OLR could be used in the various applications and climatological studies.

The contents and views expressed in this research paper are the views of the authors and do not necessarily reflect the views of their organizations.

References

Ba, M. B., Ellingson, R. G. and Gruber, A., 2003, "Validation of a technique for estimating OLR with the GOES sounder", *Journal of atmospheric and oceanic technology*, **20**, 1, 79-89.

Cheruy, F., Kandel, R. S. and Duvel, J. P., 1991, "Outgoing longwave radiation and its diurnal variation from combined ERBE and Meteosat observations: 1. Estimating OLR from Meteosat data", *Journal of Geophysical Research: Atmospheres*, **96**, D12, 22611-22622.

Ellingson, R. G. and Ferrado, R. R., 1983, "An examination of a technique for estimating the longwave radiation budget from satellite radiance observations", *Journal of climate and applied meteorology*, **22**, 8, 1416-1423.

Ellingson, R. G., Lee, H. T., Yanuk, D. and Gruber, A., 1994, "Validation of a technique for estimating outgoing longwave radiation from HIRS radiance observations', *Journal of Atmospheric and Oceanic Technology*, **11**, 2, 357-365.

Ellingson, R. G., Yanuk, D. J., Lee, H. T. and Gruber, A., 1989, "A technique for estimating outgoing longwave radiation from HIRS radiance observations", *Journal of Atmospheric and Oceanic Technology*, **6**, 4, 706-711.

Gruber, A. and Krueger, A. F., 1984, "The status of the NOAA outgoing longwave radiation data set", *Bulletin of the American Meteorological Society*, **65**, 9, 958-962.

Gruber, A. and Winston, J. S., 1978, 'Earth-atmosphere radiative heating based on NOAA scanning radiometer measurements", *Bulletin of the American Meteorological Society*, **59**, 12, 1570-1573.

Gruber, A., Ellingson, R. G., Ardanuy, P., Weiss, M., Yang, S. K. and Oh, S. N., 1994, "A comparison of ERBE and AVHRR longwave flux estimates", *Bulletin of the American Meteorological Society*, **75**, 11, 2115-2130.

Lee, H. T., Gruber, A., Ellingson, R. G. and Laszlo, I., 2007, "Development of the HIRS outgoing longwave radiation climate dataset", *Journal of Atmospheric and Oceanic Technology*, **24**, 12, 2029-2047.

Lee, H. T., Heidinger, A., Gruber, A. and Ellingson, R. G., 2004, "The HIRS outgoing longwave radiation product from hybrid polar and geosynchronous satellite observations", *Advances in Space Research*, **33**, 7, 1120-1124.

Minnis, P., Young, D. F. and Harrison, E. F., 1991, "Examination of the relationship between outgoing infrared window and total longwave fluxes using satellite data", *Journal of climate*, **4**, 11, 1114-1133.

Schmetz, J. and Liu, Q., 1988, "Outgoing longwave radiation and its diurnal variation at regional scales derived from Meteosat", *Journal of Geophysical Research: Atmospheres*, **93**, D9, 11192-11204.

Singh, R., Ojha, S. P., Kishtawal, C. M., Pal, P. K. and Kiran Kumar, A. S., 2015, "Impact of the assimilation of INSAT-3D radiances on short-rangeweather forecasts", *Q. J. R. Meteorol. Soc.*, **142**, 694, 120-131, doi:10.1002/qj.2636.

Singh, R., Singh, C., Ojha, S. P., Kumar, A. S., Kishtawal, C. M. and Kiran Kumar, A. S.,2016, "Land surface temperature from INSAT-3D imager data: Retrieval and assimilation in NWP model", *J. Geophys. Res. Atmos.*, **121**, 12, 6906-6926, doi:10.1002/2016JD024752.

Singh, R., Thapliyal, P. K., Kishtawal, C. M. and Pal, P. K., 2013, "Outgoing Longwave Radiation Product ATBD", DOI:10.19038/SAC/10/3DIMG_L2B_OLR.

Singh, R., Thapliyal, P. K., Kishtawal, C. M., Pal, P. K. and Joshi, P. C., 2007, "A new technique for estimating outgoing longwave radiation using infrared window and water vapor radiances from Kalpana very high resolution radiometer", *Geophysical Research Letters*, **34**, 23, L23815, doi:10.1029/2007GL031715.